Light & Engineering
Vol. 28, No. 6, pp. 9–16, 2020

https://doi.org/10.33383/2020-032
Svetoteknnika # 5, 2020, pp. 73–78

PHYSICAL–MATHEMATICAL MODEL OF THE INTERNAL QUANTUM EFFICIENCY DEPENDENCE ON THE CURRENT OF LEDS WITH QUANTUM WELLS

Fedor I. Manyakhin and Lyudmila O. Mokretsova

National University of Science and Technology "MISIS"
E-mail: zaomisis@yandex.ru

ABSTRACT

A physical-mathematical model of dependence of internal quantum efficiency on current for LED structures with quantum wells has been developed. The volt-ampere characteristic is modelled with the involvement of Shockley, Noyce, Sah recombination theory, supplemented by the quantum wells distribution function. In order to obtain dependence of internal quantum efficiency of LEDs on current, model of rate of ABC recombination in quantum wells is used. The developed model was tested with variations of quantum wells parameters and external impact conditions.

Keywords: LED structures with quantum wells, internal quantum efficiency, Shockley, Noyce, Sah recombination model; ABC recombination model

1. INTRODUCTION

Light emitting diodes (LEDs) with quantum wells (QW) are promising sources of light for lighting devices, full-colour displays, optrons, etc.

Quantum efficiency (QE) is one of the main parameters of LEDs QW. After commencement of serial production of LEDs based on QW hetero-structures *AlGaN*/*InGaN*/*GaN* and *AlInGaP* [1, 2], intensive studies of dependence of QE on forward-current density *J* have begun.

In one of the first works analysing behaviour of efficiency of a blue and green LED by *Lumileds Lighting* [3], it was shown that it has a maximum at J = (1–10) A · cm^{-2}. It was noted that higher values of maximum efficiency correspond to higher barrier doping and explicit periodical changes of doping density in the QW region (the modulated and doped region of QW).

According to the data of [4], with strong light excitation, when charge carriers (CC) generation rate was equal to $1.7 \cdot 10^{26}$ cm^{-3}·s^{-1}, with reduction of dislocation density from $5.7 \cdot 10^{9}$ down to $5.3 \cdot 10^{8}$ cm^{-2}, external QE (η_E) rose from 31 % up to 64 %. With that, the maximum of η_E reduces with reduction of quality of epilayers and shifts towards higher values of *J*.

Measurements of η_E at different temperatures [4, 5] have shown that, with increase of temperature of QW LED structures, the maximum of QE lowers and shifts to the range of higher *J*.

In the course of analyses of QW recombination processes, the *ABC* model [6–10] is widely used: it allows us to describe recombination rate of LED structures at different injection levels with consideration of radiative and non-radiative mechanisms:

$$R(n) = \frac{n}{\tau} = An + Bn^2 + Cn^3 + f(n), \qquad (1)$$

where R is the recombination rate, n is the excessive concentration of CC taking part in the recombination process; τ is the average CC life span; *A, B, C* are the coefficients defined experimentally for recombination rates of the Shockley-Read-Holl recombination mechanism (*A*), radiative mechanism (*B*) and the Auger mechanism (*C*). The other mechanisms of current formation are taken into account by an additional member $f(n)$.

The finer mechanisms affecting QE of QW LEDs are analysed in [11, 12] and other works, however, all the differences identified there correspond to the *ABC* model.

The analysis of literature allowed to identify that: 1) the η_E-current dependence curve of QW LED structures is bell-shaped with the maximum at $J = (1 \cdot 10^{-2}–1 \cdot 10)$ A $\cdot$ cm^{-2}; 2) the height of the maximum and its current position depends on perfection of a hetero-structure and its temperature; 3) there are still no mathematical models of the dependence of η_E and internal QE (η_I) on current and the Sah-Noyce-Shockley (SNS) model [13] (further developed in [14]) is used as the voltage-current relationship (VCR) model without taking non-uniformity of recombination rate in the space charge region (SCR) with a QW into account).

Based on the analysis, the common problem was identified: lack of the analytical model defining the relationship between VCR and lumen-voltage characteristics (LVC) for LED heterostructures based on wide-band-gap semiconductors with QW and allowing to satisfactorily describe and simulate behaviour of η_E and η_I with different external effects and distinctions of LED technological structure.

The goal of this work is to develop the analytical model of the dependence of η_I (η_E) on current on the basis of physical representation of recombination processes in QW hetero-structures.

The objectives of the work: to conduct experimental studies of VCR and η_E behaviour of QW LEDs at different temperatures and with introduction of point and continuous defects (dislocations, disordering areas); to create the physical and mathematical model of the dependence of η_E (η_I) on current; to check validity of this model with different external effects and variations of technological parameters of LED hetero-structures.

For the purpose of clarity and to prevent complication of the model, it is assumed in the work that there is a proportional relation between η_E and η_I expressed through the constant coefficient: $\eta_E = \alpha \cdot \eta_I$, $\alpha < 1$. Therefore, when modelling of QE depending on current, η_I will be meant and η_E may be derived from it by means of the coefficient α.

In the course of the model development, it is assumed that distribution of CC in quazi-neutral regions and in SCR corresponds to the Boltzmann distribution.

2. EXPERIMENT

The green, yellow and red LED's based on *AlGaN/InGaN/GaN* and *AlInGaP* hetero-structures manufactured in PCR by *Lumileds* and *Epistar* were studied. VCR, LVC and distribution of dopant over the QW region were measured at temperatures of 300 K and 373 K. Graphic representation of these characteristics is given in [15].

The blue experimental samples manufactured by *Lumileds* were marked with letter *B*, the greed samples were marked with *G* (the *InGaN/GaN* structure) and the red ones were marked with letter *R* (the *AlInGaP* structure).

VCR were measured by means of a computerised unit. The current measurement range was $(1 \cdot 10^{-7}–1 \cdot 10^{-1})$ A or $J = (1 \cdot 10^{-4}–1 \cdot 10^{2})$ A $\cdot$ cm^{-2} up to maximum voltage of 5.12 V. Forward-bias potential increment was equal to $\Delta U = (0.02 \pm 1 \cdot 10^{-4})$ V.

Dopant distribution over the QW region was measured by means of an original computerised unit [16] using the dynamic capacity method. Resolution of the dopant concentration profile depth was up to 1 nm.

Radiation was registered by the PhD 7K silicon photodiode operating in the light-to-photoelectric-current conversion mode.

In order to identify the effect of point and continuous microdefects on η_I, all LEDs were affected by reactor neutron fluxes (Φ) of 10^6, 10^7, 10^8 and 10^{15} cm^{-2} by means of the IRT 2000 installation. In the course of it, the energy spectrum and the neutron-flux density (equal to $5 \cdot 10^{10}$ cm$^{-2} \cdot$s^{-1}) were measured.

Processing of the experimental data and simulation of LED characteristics were conducted by means of *Origin 8* and *MathCad 14*.

The experimental dependences of η_E on current *I* are presented in the Figs. 1a and 2a. With temperature rising from 300 K to 373 K, the maximum of η_E reduces by (8–12)% and shifts to the range of higher values of current by more than one order of magnitude (not shown in the Figure).

More significant reduction of η_E was observed in LEDs after they being irradiated by neutrons at $\Phi = 1 \cdot 10^{15}$ cm^{-2}. The maximum of η_E reduces differently in *AlGaN/InGaN/GaN* and *AlUnGaP* structures and shifts towards higher values of current. At Φ of up to $1 \cdot 10^8$ cm^{-2}, no significant changes of the dependence $\eta_E(I)$ were observed at ambient temperature.

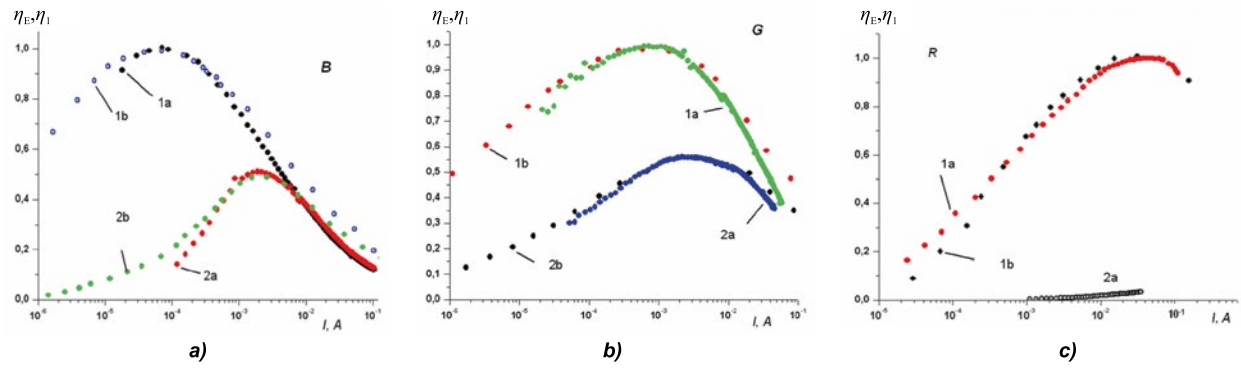

Figure. The dependences of η_E (experimental, graphs 1a, 2a) and η_I (simulated, graphs 1b, 2b) on current I for blue (*a*), green (*b*) and red (*c*) LEDs, graphs 1a and 1b are for the initial structures and are normalised to one, graph 2a is for neutron-irradiated structures, graph 2b is for model structures with concentration of radiation defects introduced in the model

The effect of neutron irradiation on lens transparency was not studied, however, no visible changes in lens transparency occurred.

The changes in distribution of charge centres of dopant in the QW region after neutron irradiation at Φ of up to 10^{15} cm^{-2} for LEDs with different quantum energy occurred in different ways. For instance, in blue and green LEDs, dopant compensation was observed only in the small region near the border of the edge of SCR of the lightly doped layer. Significant reduction of concentration of active dopant within the range of SCR changes occurred in yellow and red LEDs.

After neutron irradiation, the non ideality factor of the exponential region of VCR increased by (20–30)% and the saturation current increased by (5–6) orders of magnitude.

3. DISCUSSION

Let us assume an asymmetrical p–n^+ LED structure with uniformly doped p and n^+ layers as the model. QWs are located in the relatively slightly doped p layer within SCR without bias voltage. The QW coordinates are measured starting from the metallurgical border.

It is assumed that no tunnelling, leak currents, and other mechanisms of current formations are available other than the Shockley-Read-Holl (SRH), radiative and Auger recombination mechanisms; the Shockley diffusion mechanism [17] and SNS [13] are the main mechanisms of current formation of LED structures. With that, QWs are represented as single recombination centres with trap cross-section of σ.

CCs trapped in QWs form current, which is divided into two components: the zone-zone radiative one and the nonradiative local centre and Auger recombination component. Also, if there are point defects in the forbidden band of local levels, formation of recombination current over the entire SCR by means of the SNS mechanism is possible. Therefore, density of total recombination current J with forward bias in such structure is a particular sum:

$$J = J_{QW} + J_{rec} + j_{dif},$$

where J_{QW} is the density of quantum-well recombination current, J_{rec} is the density of recombination current through local levels of point defects in SCR, J_{dif} is the density of diffusion current of CCs that crossed the p-n^+ junction barrier and are trapped in QWs in the quazi-neutral part of the p region and within the range of operating currents of LED, $J_{rec}, J_{QW} >> J_{dif}$.

Therefore, η_E proportional to η_I is defined by the ratio between radiative and nonradiative recombination currents. The experimental results (see the Figure) witness that the coefficients of the *ABC* model vary significantly for different types of LEDs, which is pointed at by different positions of the maximums of $\eta_I(\eta_E)$ [7]. Simulation has shown that it mostly refers to the *A* and *C* coefficients.

In order to develop the model of the dependence of η_I on forward current, the SNS VCR theory was used, and it was assumed that the levels of recombination centres are located close to the centre of the forbidden band and the trap cross-sections of the electrons and holes are the same. However, as opposed to its classic description, where it is assumed that recombination centres are distributed uniformly over SCR of the symmetrical p-n structure, here it was taken into account that QWs are discretely distributed in the asymmetrical structure, i.e.

$$F_{\mathrm{QW}}(U)=$$

$$=\int_{-x_{\mathrm{n}}}^{x_{\mathrm{p}}}\frac{1}{W(U)}\cdot\frac{f_{\mathrm{QW}}(x,U)\cdot\exp\left(-\frac{\varphi_{\mathrm{k}}}{kT}\right)\left(\exp\left(\frac{qU}{kT}\right)-1\right)}{b\cdot\exp\left(-\frac{(\varphi_{\mathrm{k}}-qU)}{W(U)\cdot kT}(x-x_{\mathrm{n}})\right)+\exp\left(-\left(\frac{(\varphi_{\mathrm{k}}-qU)-\frac{(\varphi_{\mathrm{k}}-qU)}{W(U)}(x-x_{\mathrm{n}})}{kT}\right)\right)+g}dx=$$

$$=\exp\left(\frac{-\varphi_{\mathrm{k}}}{n^{*}(U)kT}\right)\cdot\exp\left[\frac{qU}{n^{*}(U)kT}-1\right]. \tag{3}$$

the recombination centres are distributed in accordance with some function $f_{\mathrm{QW}}(x, U)$. In the general case, energy levels of point defects are distributed non-uniformly too [18], in accordance with the function $f_{\mathrm{t}}(x, U)$.

With these assumptions made, the magnitude J_{QW} may be expressed as

$$J_{\mathrm{QW}}=q\sigma N_{\mathrm{QWmd}}(U)W(U)V_{\mathrm{T}}N_{\mathrm{d}}\cdot F_{\mathrm{QW}}(U)=$$

$$=q\sigma N_{\mathrm{QWmd}}(U)W(U)V_{\mathrm{T}}N_{\mathrm{d}}\times$$

$$\times\exp\left(-\frac{\varphi_{\mathrm{k}}}{n^{*}(U)kT}\right)\left[\exp\left(\frac{qU}{n^{*}(U)kT}\right)-1\right]=$$

$$=J_{\mathrm{SQW}}(U)\left[\exp\left(\frac{qU}{n^{*}(U)kT}\right)-1\right], \tag{2}$$

where, with the SNS model involved (Eq. 3),

Here $f_{\mathrm{QW}}(x, U)$ is the function of QW distribution in the relatively slightly doped layer; $N_{\mathrm{QWmd}}(U)$ is the average QW concentration in SCR depending on bias voltage U due to change in SCR width and the number of QWs in it; φ_{k} is the barrier potential;

$N_{\mathrm{QWmd}}(U)=\frac{1}{W(U)}\int_{-x_{\mathrm{n}}}^{x_{\mathrm{p}}}N_{\mathrm{QW}}(x,U)dx$; $N_{\mathrm{QW}}(x, U)$ is the QW distribution over SCR;

$f_{\mathrm{QW}}(x,U)=\frac{N_{\mathrm{QW}}(x,U)}{N_{\mathrm{QWmd}}(U)}$; $x_{\mathrm{n}}=-\frac{W(U)\cdot N_{\mathrm{a}}}{N_{\mathrm{d}}+N_{\mathrm{a}}}$;

$x_{\mathrm{p}}=\frac{W(U)\cdot N_{\mathrm{d}}}{N_{\mathrm{d}}+N_{\mathrm{a}}}$;

$W(U)=\sqrt{\frac{2\varepsilon\varepsilon_{\mathrm{o}}(N_{\mathrm{a}}+N_{\mathrm{d}})\cdot(\varphi_{\mathrm{k}}-qU)}{qN_{\mathrm{a}}N_{\mathrm{d}}}}$ is SCR width; $b = N_{\mathrm{d}}/N_{\mathrm{a}}$; $g = 2n_{\mathrm{i}}/N_{\mathrm{a}}$; N_{a} and N_{d} are the concentrations of acceptor and donor dopants.

In the expression (3), it is assumed that the front of potential barrier at the side of the n^{+} region grows linearly, therefore it is identified as $\frac{(\varphi_{\mathrm{k}}-qU)}{W(U)}(x-x_{\mathrm{n}})$ in the formula; this assumption causes virtually no impact on the nature of the model.

The coefficient $n^{*}(U)$ is defined using the formula

$$n^{*}(U)=-\frac{(\varphi_{\mathrm{k}}-qU)}{kT}\left[\ln(F_{\mathrm{QW}}(U))\right]^{-1}.$$

Given the discrete nature of QW distribution, let us write the function $f_{\mathrm{QW}}(x, U)$ as

$$f_{\mathrm{QW}}(x,U)=\frac{N_{\mathrm{QW}}(x,U)}{N_{\mathrm{QWmd}}(U)}=$$

$$=\frac{\sum_{i}\begin{pmatrix}0\mapsto x<a_{\mathrm{i}}\\(\frac{1}{H}+\beta\cdot N_{\mathrm{rec}})\mapsto a_{\mathrm{i}}\geq x\geq(a_{\mathrm{i}}+H)\\0\mapsto x>(a_{\mathrm{i}}+H)\end{pmatrix}}{N_{\mathrm{QWmd}}(U)},$$

where a_{i} is the position of the edge of the *i-th* QW relative to the metallurgical border, H is the QW width, N_{rec} is the concentration of nonradiative centres in QW, $\beta=\sigma_{\mathrm{rec}}/\sigma$ is the ratio of trap cross-section of nonradiative recombination centres to QW trap cross-section, $1/H$ is the coefficient from the condition $\frac{1}{H}\cdot\int_{\mathrm{a}}^{\mathrm{a+H}}dx=1$ (for a single recombination centre).

The current of SNS non-radiative recombination in SCR depending on U is described by the expres-

sions identical to (2) and (3). Current density J_t is expressed as

$$J_t = q\sigma_t N_{tmd}(U)W(U)V_T N_d F_t(U) = \\ = q\sigma_t N_{tmd}(U)W(U)V_T N_d \times \\ \times \exp\left(-\frac{(\varphi_k}{n_t^*(U)kT}\right)\left[\exp\left(\frac{qU}{n_t^*(U)kT}\right)-1\right] = \\ = J_{st}\left[\exp\left(\frac{qU}{n_t^* kT}\right)-1\right],$$

where $F_t(U)$ is the function identical to the function in (3), where the distribution function, $f_t(x, U)$, the sums of concentrations of initial, $N_{to}(x, U)$, and generated (by running, radiation), $N_{tr}(U)$, point defects, as well as CC trap cross-sections of defect recombination centres σ_t and σ_r therefore: $\sigma_r/\sigma_t = \gamma$, are introduced instead of QW distribution. As a result of it, $f_t(x, U)=[N_{to}(x, U) + \gamma \cdot N_{tr}(U)]/N_{tmd}(U)$, where $N_{tmd}(U)$ is the average concentration of point defects in SCR.

The exponent index coefficient $n_t^*(U)$ for $F_t(U)$ is written as

$$n_t^*(U) = -\frac{(\varphi_k - qU)}{kT}\left[\ln(F_t(U))\right]^{-1}.$$

Let us assume that radiative recombination occurs only in QW and is limited by the fraction of nonradiative flux. Therefore, it is acceptable to apply the *ABC* model for definition of η_I, and this for each *i*-th QW, since concentration of excessive CCs in QW is different at the same *U*:

$$n_{1QWi} = \exp\left(\frac{\Delta E}{n_i^*(U)\cdot kT}\right)\cdot N_d \cdot \int_{-x_n}^{x_p} F_{1QWi}(x,U)dx, \quad (4)$$

where $F_{1QW}(x, U)$ is the (3)-type function for single QW, ΔE is energy difference of forbidden bands of barrier materials and QWs.

$$f_{1QW}(x,U) = \frac{\begin{pmatrix} 0 \mapsto x < a_i \\ (\frac{1}{H} + \beta \cdot N_{rec}) \mapsto a_i \ge x \ge (a_i + H) \\ 0 \mapsto x > (a_i + H) \end{pmatrix}}{N_{1QWmd}(U)},$$

and

$$N_{1QWmd}(U) = \\ = \frac{1}{W(U)}\int_{-x_n}^{x_p}\begin{pmatrix} 0 \mapsto x < a_i \\ (\frac{1}{H} + \beta \cdot N_{rec}) \mapsto a_i \ge x \ge (a_i + H) \\ 0 \mapsto x > (a_i + H) \end{pmatrix} dx.$$

According to the three-dimensional *ABC* model, the recombination rates in the *i-th* QW are expressed by the formulae

$$R_{Si}(U) = A \cdot n_{1QWi},\ R_{Ri}(U) = B \cdot n_{1QWi}^2,$$

$$R_{Ai}(U) = C \cdot n_{1QWi}^3,$$

where $R_{Si}(U)$, $R_{Ri}(U)$ and $R_{Ai}(U)$ are the recombination rates of SRH, zone-zone and Auger mechanisms in the same *i*-th QW respectively; *A, B* and *C* are the *ABC* model coefficients. With that, the principle of equality of recombination fluxes as per SNS and the *ABC* model shall be met.

The QW regions are essentially two-dimensional. Therefore, concentration of excessive CCs calculated using (4) and measured in cm^{-3} for QW shall be assumed equal to two-dimensional concentration of CC, i.e. (4) shall be multiplied by QW width *H* and the coefficients *A, B* and *C* shall be normalised to the two-dimensional *ABC* model [19]. Then η_I depending on concentration of excessive charge carriers in QWs may be expressed by the formula

$$\eta_I = \frac{B \cdot \sum_i \left(Hn_{1QWi}\right)^2}{\left[A \cdot \sum_i \left(Hn_{1QWi}\right) + J_t / q\right] + \\ + B \cdot \sum_i \left(Hn_{1QWi}\right)^2 + C \cdot \sum_i \left(Hn_{1QWi}\right)^3}, \quad (5)$$

where the *A, B, C* coefficients correspond to the two-dimensional model.

The dependence of η_I on current is defined by dependence of excessive concentration on current and the dependence of external quantum efficiency *L* on *J* is described as

$$L(J) = \alpha \cdot \frac{J}{q} \cdot \eta_I.$$

In (5), nonradiative recombination rate in barriers between QWs is expressed by the relation $J_t / q = A_t \cdot n_t$, where A_t is the *ABC*-model coefficient for the SRH recombination mechanisms in regions between QWs and n_t is effective concentration

Table 1. LED Model Parameters

Sample of LED	Donor concentration, N_d, cm^{-3}	Acceptor concentration, N_a, cm^{-3}	QW width, nm	Barrier width, nm	Position of the first QW, a_1, nm
B (5 QWs)	$2 \cdot 10^{19}$	$7 \cdot 10^{18}$	3.0	12	5.2
G (5 QWs)	$2 \cdot 10^{19}$	$8 \cdot 10^{17}$	3.0	12	4.5
R (8 QWs)	$2 \cdot 10^{18}$	$8 \cdot 10^{17}$	2.5	7.5	2.0

Table 2. Model Coefficients *A, B, C* and Parameters of the Dependences η_I for Initial LED Samples

Sample of LED	A, s^{-1}	B, cm^2·s^{-1}	C, cm^4· s^{-1}	n_{max}, cm^{-2} at 300 K (model)	I_{max}, A		η_{Imax}	
					T = 300 K	T = 373 K	T = 300 K	T = 373 K
B (5 QWs)	$1 \cdot 10^4$	$8 \cdot 10^{-6}$	$1 \cdot 10^{-15}$	$1.5 \cdot 10^8$	$7.1 \cdot 10^{-5}$	$1.3 \cdot 10^{-3}$	1.0	0.93
G (5 QWs)	$3 \cdot 10^4$	$8 \cdot 10^{-6}$	$4 \cdot 10^{-19}$	$9 \cdot 10^{12}$	$7.2 \cdot 10^{-4}$	$1.0 \cdot 10^{-2}$	1.0	0.94
R (8 QWs)	$8 \cdot 10^6$	$4 \cdot 10^{-5}$	$8 \cdot 10^{-20}$	$1 \cdot 10^{13}$	$4.6 \cdot 10^{-2}$	$2.5 \cdot 10^{-1}$	1.0	0.90

of CCs at an energy level $(\varphi_k - qU)/(n_t^* k)$ (effective level of CC flow to the recombination region).

CONCLUSION

The presented model was tested by exposure to temperatures ranging between –200 K and 500 K and neutron Φ ranging between 10^6 and 10^{15} cm^{-2}, by degree of QW region doping ranging between $1 \cdot 10^{17}$ and $7 \cdot 10^{18}$ cm^{-3} as well as by QW coordinates and width. The model dependences η_I without consideration of the fourth member of $f(n)$ in (1) are presented in the Figs. 1b and 2b. The model parameters are summarised in Table 1. The parameters of semiconductors for the models were taken from [20].

The variations of the model parameters have shown that the dependence of η_I on current is primarily influenced by QW position relative to the metallurgical border, degree of doping of the *p* and *n* regions, initial width of SCR and depth of QWs. To the lesser extent the position of the maximum η_I and its values are influenced by QW width.

In order to obtain satisfactory fit of the results of modelling of η_I, the coefficients of the two-dimensional *ABC* model [19] were selected and the features of interaction between neutrons and semiconductors were taken into account: cross-section of neutron and atom interaction, formation of tracks, etc. Concentration of point defects formed by neutrons was calculated using the formula [21, p. 27].

$$N_{tr} = \Phi N_i \sigma_d \bar{\nu},$$

where Φ is the neutron fluence, N_i is the number of atoms in a unit of semiconductor volume, σ_d is the collision cross-section, $\bar{\nu}$ is the average number of shifted atoms per one primarily displaced atom.

$\bar{\nu}$ equals approximately to $3 \cdot 10^2$ per one incident neutron. Since neutron collides with the atom core, σ_d is taken approximately equal to $1 \cdot 10^{-24}$ cm^2. The disordering area after collision between a neutron and a primary atom is about (50–60) nm [21].

The model coefficients *A, B* and *C* for the two-dimensional *ABC* model are presented in Table 2. For the red LED (*R*), modelling was not conducted in the case of neutron irradiation at $\Phi = 1 \cdot 10^{15}$ cm^{-2} due to significant reduction of η_I which is apparently related to formation of tunneling current due to formation of large disordering areas comparable with QW repetition period.

In Table 2, n_{max} and I_{max} are the values of excessive concentration of CC and current at the maximum value of η_I (η_{Imax}) normalised to one.

The rate of nonradiative SRH recombination and, therefore, the coefficients A and A_t are largely influenced by degree of perfection of QW crystal structure [4].

The main conclusions are the next:

1. The physical and mathematical model of dependence of internal quantum efficiency of QW LED on current was developed using the SRH and *ABC* recombination models; the QW distribution function was introduced in the SNS model and the *ABC* model was applied for identification of rates of radiative and nonradiative recombination in QWs.

2. Due to low QW width, to calculated their recombination rate using the *ABC* model, it is necessary to use the numeric value of CC concentration as two-dimensional concentration of excessive charge carriers and the relevant coefficients *A, B* and *C* normalised to the two-dimensional model.

ACKNOWLEDGMENTS

The work is conducted under the state grant provided within the Programme of Competitive Growth of NITU MISiS among the World's Leading Research Centres for 2013–2020.

REFERENCES

1. Nakamura, S., Iwasa, M.S. Method of manufacturing p-type compound semiconductors // Patent N5306662. Apr.1994. Japan.

2. Amano, H., Akasaki, I. et.al. Method for producing a luminous element of III-group nitride. Patent #5496766. Mar. 1996. Japan.

3. Mamakin, S.S., Yunovich, A.E., Vattana, A.B., Manyakhin, F.I. Electric Properties and Fluorescence Spectra of LED's Based on InGaN/GaN Heterojunctions with Modulated and Doped Quantum Wells [Elektricheskiye svoystva i spektry luminestsentsii svetodiodov na osnove geteroperekhodov InGaN/GaN s modulirovanno-legirovannymi kvantovymi yamami] // FTP, 2003, Vol. 37, # 9, pp. 1131–1137.

4. Voytsekhovsky, A.V., Nesmelov, S.N., Kulchitsky, N.A., Melnikov, A.A. The Influence of Dislocations on Internal Quantum Efficiency of Light-Emitting Structures Based on InGaN/GaN Quantum Wells [Vliyaniye dislokatsiy na vnutrennyuyu kvantovuyu effektivnost svetoizluchayushchikh struktur na osnove kvantovykh yam InGaN/GaN] // Nano i mikrosistemnaya tekhnika, 2011, Vol. 8η_I, pp. 27–35.

5. Shim, J.-I., Shin, D.-S. Measuring the internal quantum efficiency of light-emitting diodes towards accurate reliable room-temperature characterization // Nanophotonics, 2018, September, pp. 1–15.

6. Zang, M., Bhattacharya, P., Singh, J., Hinckley, J. Direct measurement of auger recombination in $In_{0.1}Ga_{0.9}N$/GaN quantum well and its impact on the efficiency in $In_{0.1}Ga_{0.9}N$/GaN multiply uantum well light emitting diodes // Appl. Phys. Letter, 2009, Vol. 95, # 20, pp. 1108.

7. Dai, Q., Shan, Q., Wang, J., Chhajed, S., Cho, J.M., Shubert, E.F., Crawford, M.H., Koleske, D. D., Kim, M.-H., Park, Y. Carrier recombination mechanisms and efficiency droop in GaInN/GaN light-emitting diodes // Appl. Phys. Letter, 2010, Vol. 97, # 13, pp. 3507.

8. David, A., Grundmann, M.J. Droop in InGaN light-emitting diodes: A differential carrier lifetime analysis // Appl. Phys. Letter, 2010, Vol. 96, # 10, pp. 3504.

9. David, A., Hurni, C.A., Young, N.G., Craven, M.D. Electrical properties of III-nitride LEDs recombination-based injection model and theoretical limits to electrical efficiency and electroluminescent cooling // Appl. Phys. Letter, 2016, Vol. 109, # 8, pp. 3501.

10. Hopkins, M.A., Allsopp, D.W.E., Kappers, M.J., Oliver, R.A., Humpreys, C.J. The ABC model of recombination reinterpreted: Impact on understanding carrier transport and efficiency droop in InGaN/GaN light emitting diodes // J. Appl. Phys. 2017, Vol. 122, # 23, pp. 4505.

11. Bochkaryova, N.I., Rebane, Yu.T. Shreter, Yu.G. Growth of Shockley-Reed-Hall Recombination Rate in InGaN/GaN Quantum Wells as the Major Mechanism of Loss of LED Efficiency at High Injection Levels [Rost skorosti rekombinatsii Shokli-Rida-Holla v kvantovykh yamakh InGaN/GaN kak osnovnoy mekhanizm padeniya effektivnosti svetodiodov pri vysokikh urovnyakh inzhektsii] // FTP, 2015, Vol. 49, # 12, pp. 1714–1719.

12. Prudaev, I.A., Skakunov, M.S., Lelekov, M.A., Ryaboshtan, Yu.L., Gorlachuk, P.V., Marmalyuk, A.A. Recombinant Currents in LEDs Based on Multiple Quantum Wells $(Al_xGa_{1-x})_{0.5}In_{0.5}P/(Al_yGa_{1-y})_{0.5}In_{0.5}P$ [Rekombinatsyonnyye toki v svetodiodakh na osnove mnozhestvennykh kvantovykh yam (AlxGa1-x)0.5In0.5P/(AlyGa1-y)0.5In0.5P] // Izvestiya vuzov. Fizika, 2013, Vol. 56, # 8, pp. 44–47.

13. Sah C.T., Noyce R.N., Shockley W. Carrier Generation and Recombination in P-N Junctions and P-N Junction Characteristics // Proc. IRE, 1957, Vol. 45, pp. 1228–1243.

14. Choo, S.C. Carrier generation-recombination in the space-charge region of an assymmetrical p-n junction // Solid State Electronics,1968, Vol. 11, pp. 1069–1077.

15. Fedor I. Manyakhin, Arthur B. Vattana, and Lyudmila O. Mokretsova Application of the Sah-Noyce-Shockley Recombination Mechanism to the Model of the Voltage-Current Relationship of LED Structures with Quantum Wells// Light & Engineering Journal, 2020, Vol. 28, #5, pp. 31–38.

16. Goryunov, N.N., Manyakhin, F.I., Klebanov, M.P., Lukashev, N.V. Impulse Three-Frequency Method of Measurement of Charged Centre Parameters in the Space Charge Region of Semiconductor Structures [Impulsnyy tryokhchastotnyy metod izmereniya parametrov zaryazhennykh tsentrov v oblasti prostranstvennogo zaryada

poluprovodnikovykh struktur] // Pribory i sistemy upravleniya, 1999, Vol. 10, pp. 46–49.

17. Shockley, W. The Theory of p – n Junctions in Semiconductors and p-n Junction Transistors // Bell Syst. Tec. J. 1949, Vol. 28, pp. 435–489.

18. Abdullaev, Zh.S., Gusev, M. Yu., Zyuganov, A.N., Torchinskaya, T.V. Parameters of Deep Centres in AlGaAs LEDs Evaluated by Capacity and Injection Spectroscopy Methods [Parametry glubokikh tsentrov v svetodiodakh AlGaAs otsenyonnyye metodami emkostnoy i inzhektsionnoy spektroskopii] // Ukr. Phys. Journal. 1989, Vol. 34, # 8, pp. 1220–1224.

19. Voytsekhovky, A.V., Gorn, D.I. Recombination Mechanisms in InGaN/GaN Structures with Quantum Wells at High Levels of Excitation [Mekhanizmy rekombinatsii v strukturakh InGaN/GaN s kvantovymi yamami pri vysokikh urovnyakh vozbuzhdeniya] // Izvestiya vuzov. Fizika, 2015, Vol. 58, # 8/2, pp. 171–173.

20. NSM Archive. Physical Properties of Semiconductors. URL: http://www.ioffe.rssi.ru/SVA/NSM/Semicond/ (reference date: 28.02.2020).

21. Ladygin, E.A. The Effect of Ionising Radiation on Electronic Equipment [Deystviye pronikayushchey radiatsii na izdeliya elektronnoy tekhniki]. Moscow: Sovetskoye radio, 1980, 224 p.

Fedor I. Manyakhin,
Doctor of Physical and Mathematical Sciences, Professor. In 1973, he graduated from the Moscow Institute of Electronic Engineering (MIEM). At present, he is a Professor of the Automatic Design sub-department of NITU MISIS, author and co-author of more than 150 publications, awarded with the diploma of the Ministry of Education and Science of Russia, prize winner of the Golden Names of Higher Education 2018 contest in nomination of Contribution to Science and Higher Education. His research interests: semiconductor electronics, physics of semiconductor devices

Lyudmila O. Mokretsova,
Associate Professor, Ph.D. in Technical Sciences. In 1978, she graduated from the Moscow Institute of Steel and Alloys (MISIS). At resent, she is Associate Professor of the Automatic Design sub-department of NITU MISIS, prize winner of the Golden Names of Higher Education 2018 contest in nomination of Introduction of Innovative Teaching Techniques. Her research interests: 3D modelling in light design